Relativistic study of $E1$ and $M1$ transitions in the boron isoelectronic sequence

Mina Vajed-Samii, Dinh Ton-That,* and Lloyd Armstrong, Jr.
Department of Physics, The Johns Hopkins University, Baltimore, Maryland 21218
(Received 24 November 1980)

The relativistic transition energies and electric-dipole oscillator strengths in length and velocity forms are calculated for ions of the boron sequence. Transitions from the $2s2p^2$, $J = 1/2$, $3/2$, and $5/2$ excited states to the $2s^22p$, $J = 1/2$ and $3/2$ levels of the ground state are considered. The magnetic-dipole transition studied relativistically is that between the $J = 1/2$ and $3/2$ levels of the ground state. The trends in the relative importance of relativistic contributions and correlation effects along the isoelectronic sequence for the different transitions are discussed. A more detailed study of the various effects contributing to the excitation energies and oscillator strengths of Fe XXII, and comparison with other available results for this ion is carried out.

I. INTRODUCTION

The increasing interest in excitation energies and oscillator strengths of transitions in highly ionized atoms in recent years[1-9] can be attributed to two main factors. First, there is increased availability of experimental data for highly ionized systems obtained from beam-foil experiments[10] and astrophysical measurements.[11] Second, the calculated results are useful, especially in the case of yet unobserved transitions, for application to various other related fields such as determining the density and temperature of the solar corona[11] or making diagnostic studies of thermonuclear plasmas.[12]

In evaluating transition energies and oscillator strengths in many electron systems, electron-electron interaction effects play a very important role and must be considered. Furthermore, as we progress along an isoelectronic sequence, the nuclear charge increases and thus relativistic effects become increasingly important. Therefore in studying transitions in atoms and ions, it is advantageous to use a method which treats both relativistic and correlation effects in a first principle manner. Such techniques have been developed and applied to several sequences.[2-8] The relativistic multiconfigurational Dirac-Hartree-Fock (MCDHF) is such a procedure and can, in principle, treat all correlation and relativistic effects simultaneously.

The relativistic MCDHF has been successfully applied to the study of transitions in some simple sequences[2] as well as in the isoelectronic sequences of some rare-gas atoms.[4] In all of these cases the active shells are always either filled or have one electron outside a closed shell. It has been found that for the sequences isoelectronic with the small atoms, relativistic effects are generally similar to those seen in hydrogenic atoms[2,3] while in the larger systems these effects are large and deviate from the hydrogen-atom predictions at high Z, especially for the $\Delta n = 0$ transitions.[4] Correlation effects were found to be important, as demonstrated by their role in bridging the gap between the results obtained using the length and velocity forms of the electric-dipole transition operator.[1,2,4]

The ionic-sequence isoelectronic with the boron atom is of special interest and has been the subject of several investigations lately.[5-7,9] The ions of the boron sequence, although containing only a few electrons, can have three electrons in open shells in the excited state and therefore are expected to manifest more complex behavior as a result of electron-electron interaction effects. Besides the study by Cheng *et al.*[9] of all the transitions between $n = 2$ states in the sequences of all first-row atoms, two detailed multiconfigurational studies of the boron sequence have been carried out. In the first, Dankwort and E. Trefftz[6] study the transitions in ions up to Fe XXII, and in the second, Glass[7] gives a detailed analysis of the results in Fe XXII.

In the present work, we study the boron isoelectronic sequence using the relativistic multiconfiguration procedure. Special emphasis is placed on the roles of electron-electron interaction and relativistic effects and also on their interplay in the intermediate and high-Z region. We have used a limited number of configurations in studying the various ions of the sequence but have investigated the role of adding more configurations in the case of one of the electric-dipole transitions in iron. In Sec. II we shall briefly discuss our procedure for obtaining the wave functions for the ground and excited states and for evaluating the transition matrix elements. We then describe our results. Section III contains analysis of the different results obtained for the boron sequence, along with a discussion of the trends observed in going through the isoelectronic sequence. In Sec. III we also report on the results obtained for Fe XXII and their improvement

TABLE I. Weight coefficients for the relativistic configurations belonging to the $J=\frac{1}{2}$ and $\frac{3}{2}$ levels of the ground state of ions in the boron sequence. Numbers in parentheses are multiplicative powers of ten.

Element \ State	$J=\frac{1}{2}$ $2s^2 2p_{1/2}$	$(^2P^0_{1/2})$ $2p_{1/2}2p^2_{3/2}$	$2s^2 2p_{3/2}$	$J=\frac{3}{2}$ $2p_{1/2}2^1_2{}^2_{3/2}$	$(^2P^0_{3/2})$ $2p^3_{3/2}$	$2p^2_{1/2}2p_{3/2}$
B	0.9725	0.233	−0.9727	−0.2304 (−3)	0.1618	−0.1662
Ne^{5+}	0.9815	0.1912	−0.9814	−0.6585 (−4)	−0.1351	−0.1363
S^{11+}	0.9848	0.1740	−0.9842	−0.2724 (−3)	−0.1224	−0.1278
Ar^{13+}	0.9856	0.1689	−0.9849	−0.3818 (−3)	−0.1187	−0.1263
Ti^{17+}	0.9874	0.1580	−0.9861	−0.6577 (−3)	−0.1106	−0.1243
Fe^{21+}	0.9893	0.1456	−0.9872	−0.9819 (−3)	−0.1014	−0.1229
Kr^{31+}	0.9939	0.1102	−0.9898	−0.1693 (−2)	−0.7562 (−1)	−0.1204
Mo^{37+}	0.9960	0.8930 (−1)	−0.9910	−0.1876 (−2)	−0.6084 (−1)	−0.1188
W^{69+}	0.9997	0.2540 (−1)	−0.9945	−0.9157 (−3)	−0.1708 (−1)	−0.1029

and compare them to those obtained by other authors. Section IV contains our main conclusions.

II. PROCEDURE AND RESULTS

A. Wave functions

The relativistic multiconfiguration Dirac-Hartree-Fock program of Desclaux[13] is used to generate the wave functions for the ground and excited states of the boron isoelectronic sequence. The wave functions are obtained by including all configurations formed by orbitals with principal quantum number $n=2$. Each state (ground or excited) is obtained independently in a self-consistent manner. In the relativistic formalism each state is labeled by the quantum number representing its total orbital angular momentum J. If two states with the same electronic configuration have the same J, then these levels will be further classified according to the ordering of their energy levels.

The nonrelativistic $2s^2 2p$ ground state of the ions in the boron sequence is split into $J=\frac{1}{2}$ and $\frac{3}{2}$ states when relativistic effects are taken into account. The $J=\frac{1}{2}$ state in our calculation is expressed as a mixture of the two configurations $1s^2 2s^2 2p_{1/2}$ and $1s^2 2p_{1/2}2p^2_{3/2}$; while the $J=\frac{3}{2}$ level can be formed by a combination of the four configurations, $1s^2 2s^2 2p_{3/2}$, $1s^2 2p_{1/2}(2p^2_{3/2}; J=2)$, $1s^2 2p^3_{3/2}$, and $1s^2 2p^2_{1/2}2p_{3/2}$. These states are, respectively, equivalent to the $^2P^0_{1/2}$ and $^2P^0_{3/2}$ in the nonrelativistic formalism. In Table I we list the weight of each configuration for the two ground-state levels of a few sample elements in the boron isoelectronic sequence.

The excited states considered all have the $1s^2 2s 2p^2$ electronic structure and can be categorized according to their total angular momentum into three groups, the $J=\frac{1}{2}$, $\frac{3}{2}$, and $\frac{5}{2}$ states. There are three $J=\frac{1}{2}$ levels which are generated from the linear combination of the three relativistic configurations, $1s^2 2s 2p^2_{1/2}$, $1s^2 2s 2p_{1/2}2p_{3/2}$ and $1s^2 2s(2p^2_{3/2}; J=0)$, three $J=\frac{3}{2}$ levels which are obtained from the mixture of $1s^2 2s(2p^2_{3/2}; J=2)$, $1s^2(2s 2p_{1/2}; J=0)2p_{3/2}$, and $1s^2(2s 2p_{1/2}; J=1)2p_{3/2}$ configurations, and two $J=\frac{5}{2}$ levels obtained from the combination of the $1s^2(2s 2p_{1/2}; J=1)2p_{3/2}$ and $1s^2 2s(2p^2_{3/2}; J=2)$ relativistic configurations. For a particular J, the level will be referred to as lowest, middle, or highest, according to the value of the total energy associated with it. In Tables II and III we list the configurations and their corresponding weights for the various levels of

TABLE II. Coefficients for the configurations of the $J=\frac{1}{2}$ excited states of B sequence; (a): $2s 2p^2_{1/2}$; (b): $(2s 2p_{1/2}; J=1)\ 2p_{3/2}$; (c): $2s(2p^2_{3/2}; J=0)$.

Element \ State	Highest $J=\frac{1}{2}$ (a)	(b)	(c)	Middle $J=\frac{1}{2}$ (a)	(b)	(c)	Lowest $J=\frac{1}{2}$ (a)	(b)	(c)
B	−0.444	−0.814	0.376	0.577	0.000	0.816	0.667	−0.577	−0.471
Ne^{5+}	−0.450	−0.817	0.361	0.585	0.028	0.810	0.672	−0.576	−0.466
Ar^{13+}	−0.215	−0.744	0.632	−0.666	−0.334	−0.667	0.708	−0.565	−0.425
Ti^{17+}	0.0321	0.603	−0.798	0.667	0.576	0.473	−0.744	0.548	0.384
Fe^{21+}	0.061	−0.470	0.881	0.609	0.718	0.338	−0.791	0.516	0.330
Kr^{31+}	0.088	−0.258	0.962	0.398	0.895	0.201	−0.913	0.366	0.182
Mo^{37+}	0.071	−0.179	0.981	0.280	0.948	0.152	−0.957	0.265	0.118
W^{69+}	0.015	−0.038	0.999	−0.049	−0.998	−0.032	0.999	−0.049	−0.168

TABLE III. Coefficients for the configurations of $J=\frac{3}{2}$ excited state of B sequence; (a): $2s2p^2_{3/2}$; (b): $(2s2p_{1/2}; J=0)2p_{3/2}$; (c): $(2s2p_{1/2}; J=1)2p_{3/2}$. Number in parentheses are multiplicative powers of ten.

Element \ State	Highest $J=\frac{3}{2}$ (a)	(b)	(c)	Middle $J=\frac{3}{2}$ (a)	(b)	(c)	Lowest $J=\frac{3}{2}$ (a)	(b)	(c)
B	0.730	0.183	0.658	0.574	−0.643	−0.507	0.333	0.745	0.577
Ne^{5+}	0.751	0.163	0.640	−0.572	0.645	0.507	−0.330	−0.747	0.577
S^{11+}	0.776	0.146	0.614	−0.548	0.641	0.538	−0.315	−0.754	0.577
Ar^{13+}	0.790	0.136	0.598	−0.532	0.638	0.556	−0.307	−0.758	0.576
Ti^{17+}	0.827	0.108	0.552	−0.487	0.632	0.603	−0.284	−0.768	0.575
Fe^{21+}	0.870	0.737	0.487	0.424	−0.622	−0.659	−0.255	−0.779	0.572
Kr^{31+}	0.955	0.357 (−2)	0.296	0.243	−0.587	−0.772	−0.172	−0.809	0.562
Mo^{37+}	0.978	0.128 (−1)	0.208	0.164	−0.569	−0.806	−0.129	−0.822	0.554
W^{69+}	0.999	−0.842 (−2)	0.396 (−1)	−0.788 (−1)	0.546	0.834	0.281 (−1)	0.848	−0.530

the $J=\frac{1}{2}$ and $\frac{3}{2}$ excited states of ions of the boron isoelectronic sequence. Here, as in Table I, only a few of the elements studied have been chosen for listing since they will suffice for showing the general trends for the sequence which will be discussed in Sec. III.

B. Energies and transitions

Using the self-consistently obtained relativistic multiconfigurational wave functions described in Sec. II A, we obtain the total energy of each state, including the correlation energy contribution of all $n=2$ orbitals. The Breit interaction is included in first-order perturbation theory in its configuration-average form.[14] The transition energy is then simply the difference between the total energy of an excited state and that of the ground state; for the ions of the boron sequence transition energies are listed (in atomic units) in Tables IV–IX for the different transitions considered.

The form of the electromagnetic transition operators in the relativistic formalism has been discussed earlier in the literature[1,2] and we shall only mention those points that are of particular interest in the present case. For the electric-dipole transitions between the various excited states with $J=\frac{1}{2}$, $\frac{3}{2}$, or $\frac{5}{2}$, and the ground states ($J=\frac{1}{2}$ or $\frac{3}{2}$), we have used two forms of the operator corresponding to the two relativistic gauges: the Coulomb gauge which, in the nonrelativistic theory reduces to the velocity form of the operator, and a second gauge which, in the nonrelativistic formalism is equivalent to the length gauge. It has been shown[1] that, if the two states connected by the transition operator are exact solutions of the same Hamiltonian, the use of the two different gauges should produce identical results. However, since our wave functions are not exact and have been obtained by the MCDHF procedure using a finite number of configurations, a different value is obtained for the transition oscillator strength, depending upon which gauge is used. By using both forms of the dipole operator and comparing the results obtained for the oscillator strength of a transition, we hope to gain further

TABLE IV. Transition energies and oscillator strengths for the emission of one photon in transition from the $J=\frac{1}{2}$ excited states to $J'=\frac{1}{2}$ ground state of B sequence. Numbers in parentheses are multiplicative powers of ten.

Z	Element \ Transition	Highest $J=\frac{1}{2}\rightarrow J'=\frac{1}{2}(^2P^0_{1/2})$ ΔE(a.u.)	f_l	Middle $J=\frac{1}{2}\rightarrow J'=\frac{1}{2}(^2P^0_{1/2})$ ΔE(a.u.)	f_l	Lowest $J=\frac{1}{2}\rightarrow J'=\frac{1}{2}(^2P^0_{1/2})$ ΔE(a.u.)	f_l
5	B	0.3835	0.4549	0.3159	0.1540	0.1133	0.250 (−7)
10	Ne^{5+}	1.1912	0.1688	1.0755	0.0652	0.4327	0.250 (−7)
14	Si^{9+}	1.8346	0.9661 (−1)	1.6994	0.573 (−1)	0.7094	0.200 (−6)
16	S^{11+}	2.1747	0.6922 (−1)	2.0293	0.623 (−1)	0.8602	0.448 (−4)
18	Ar^{13+}	2.5388	0.4481 (−1)	2.3746	0.713 (−1)	1.0229	0.903 (−4)
22	Ti^{17+}	3.3905	0.1397 (−1)	3.1139	0.835 (−1)	1.3930	0.299 (−3)
23	V^{18+}	3.6392	0.1022 (−1)	3.3107	0.836 (−1)	1.4962	0.399 (−3)
26	Fe^{21+}	4.4992	0.4151 (−2)	3.9438	0.802 (−1)	1.8337	0.796 (−3)
28	Ni^{23+}	5.1872	0.2378 (−2)	4.4132	0.770 (−1)	2.0815	0.121 (−2)
36	Kr^{31+}	9.2823	0.3242 (−3)	6.9248	0.663 (−1)	3.2207	0.399 (−2)
42	Mo^{37+}	14.4530	0.7950 (−4)	9.8759	0.625 (−1)	4.1726	0.631 (−2)
54	Xe^{49+}	33.9964	0.4573 (−5)	20.5515	0.661 (−1)	6.2651	0.864 (−2)
74	W^{69+}	119.7242	0.5031 (−7)	65.6128	0.951 (−1)	10.8865	0.864 (−2)

TABLE V. Energies and oscillator strengths of $2s2p^2$; $J=\frac{1}{2}$ to $2s^22p$; $J'=3/2$ emission for B sequence. Numbers in parentheses are multiplicative powers of ten.

Z	Element \ Transition	Highest $J=\frac{1}{2}\rightarrow J'=\frac{3}{2}(^2P^0_{3/2})$ ΔE(a.u.)	f_l	Middle $J=\frac{1}{2}\rightarrow J'=\frac{3}{2}(^2P^0_{3/2})$ ΔE(a.u.)	f_l	Lowest $J=\frac{1}{2}\rightarrow J'=\frac{3}{2}(^2P^0_{3/2})$ ΔE(a.u.)	f_l
5	B	3.814 (−1)	2.600 (−1)	3.139 (−1)	3.101 (−1)	1.113(−1)	1.487 (−6)
10	Ne^{5+}	1.184	9.475 (−2)	1.068	1.127 (−1)	4.261 (−1)	2.093 (−6)
14	Si^{9+}	1.802	7.863 (−2)	1.667	5.989 (−2)	6.770 (−1)	1.603 (−5)
16	S^{11+}	2.114	7.987 (−2)	1.969	3.962 (−2)	8.001 (−1)	3.367 (−5)
18	Ar^{13+}	2.435	8.288 (−2)	2.271	2.180 (−2)	9.196 (−1)	6.208 (−5)
22	Ti^{17+}	3.135	8.106 (−2)	2.858	2.427 (−3)	1.137	1.551 (−4)
23	V^{18+}	3.327	7.887 (−2)	2.999	9.898 (−4)	1.184	1.843 (−4)
26	Fe^{21+}	3.962	7.143 (−2)	3.407	3.021 (−5)	1.297	2.732 (−4)
28	Ni^{23+}	4.443	6.684 (−2)	3.669	4.412 (−4)	1.337	3.205 (−4)
36	Kr^{31+}	7.047	5.479 (−2)	4.689	2.889 (−3)	9.856 (−1)	2.442 (−4)
42	Mo^{37+}	1.007 (+1)	5.127 (−2)	5.498	4.213 (−3)	−2.051 (−1)	−3.781 (−5)
54	Xe^{49+}	2.085 (+1)	5.324 (−2)	7.411	5.227 (−3)	−6.875	−5.847 (−4)
74	W^{69+}	6.599 (+1)	7.410 (−2)	1.188 (+1)	4.994 (−3)	−4.283 (+1)	−1.170 (−3)

insight into the nature of various effects such as core polarization and correlation effects.

The oscillator strength for the electric-dipole transitions under consideration are listed in Tables IV–VIII for ions of the boron isoelectronic sequence. In these tables we have only listed the oscillator strengths obtained by using the gauge which reduces to the nonrelativistic dipole length form. The reason for listing only this set of results, as will be further discussed in Sec. III C, is that it seems to be the more stable one under small changes in the wave function. It should be noted that in our calculations of the f values, we take into account the effect of the nonorthogonality of the core and valence s electrons from the ground and excited state by including exchange-overlap matrix elements.[15] One example of such a transition matrix element is

$$\langle 1s|1s\rangle\langle 2s|2s\rangle\langle 2s|1s\rangle\langle 2p_{1/2}|2p_{1/2}\rangle\langle 1s|\mathrm{op}|2p_{1/2}\rangle,$$

which includes one order of the $2s,1s$ exchange-overlap integral and arises in the transition between the configurations $1s^22s^22p_{1/2}$ of the ground state and $1s^22s\,2p^2_{1/2}$ of the excited state. The contribution from terms having two orders of the overlap integral is much smaller and can be neglected. In first order, however, these exchange-overlap terms have modified the value of the oscillator strength by 4 to 28% in the case of the Be-isoelectronic sequence.[15] Thus, this is a real and sizable effect and must be included in all calculations where the core orbitals are generated self-consistently, in an independent way for each of the ground and excited states.

TABLE VI. Energies and oscillator strengths for the transition from the $J=\frac{3}{2}$ excited states to $J'=\frac{1}{2}$ ground state. Numbers enclosed by parentheses are multiplicative powers of ten.

Z	Element \ Transition	Highest $J=\frac{3}{2}\rightarrow J'=\frac{1}{2}(^2P^0_{1/2})$ ΔE(a.u.)	f_l	Middle $J=\frac{3}{2}\rightarrow J'=\frac{1}{2}(^2P^0_{1/2})$ ΔE(a.u.)	f_l	Lowest $J=\frac{3}{2}\rightarrow J'=\frac{1}{2}(^2P_{1/2})$ ΔE(a.u.)	f_l
5	B	3.843 (−1)	1.240 (−1)	2.494 (−1)	1.320(−1)	1.33 (−1)	7.511 (−11)
10	Ne^{5+}	1.195	4.334 (−2)	8.460 (−1)	5.389 (−2)	4.345 (−1)	4.497 (−8)
14	Si^{9+}	1.854	2.784 (−2)	1.343	3.843 (−2)	7.199 (−1)	4.068 (−7)
16	S^{11+}	2.208	2.318 (−2)	1.612	3.466 (−2)	8.808 (−1)	9.111 (−7)
18	Ar^{13+}	2.589	1.950 (−2)	1.902	6.466 (−2)	1.060	1.819 (−6)
22	Ti^{17+}	3.469	1.379 (−2)	2.570	3.046 (−2)	1.495	5.697 (−6)
23	V^{18+}	3.722	1.259 (−2)	2.760	3.040 (−2)	1.624	7.289 (−6)
26	Fe^{21+}	4.591	9.427 (−3)	3.400	3.090 (−2)	2.077	1.417 (−5)
28	Ni^{23+}	5.282	7.651 (−3)	3.894	3.163 (−2)	2.442	2.090 (−5)
36	Kr^{31+}	9.385	3.044 (−3)	6.597	3.612 (−2)	4.622	7.059 (−5)
42	Mo^{37+}	1.457 (+1)	1.528 (−3)	9.710	4.060 (−2)	7.345	1.348 (−4)
54	Xe^{49+}	3.417 (+1)	4.705 (−4)	2.063 (+1)	5.333 (−2)	1.748 (+1)	3.288 (−4)
74	W^{69+}	1.200 (+2)	1.097 (−4)	6.591 (+1)	8.7581 (−2)	6.140 (+1)	8.280 (−4)

TABLE VII. Energies and oscillator strengths for the $J=\frac{3}{2}$ excited states to $J'=\frac{3}{2}$ ground-state transition of B sequence. Numbers enclosed by parentheses indicate multiplicative powers of ten.

Z	Element \ Transition	Highest $J=\frac{3}{2}\rightarrow J'=\frac{3}{2}(^2P^0_{3/2})$ ΔE (a.u.)	f_l	Middle $J=\frac{3}{2}\rightarrow J'=\frac{3}{2}(^2P^0_{3/2})$ ΔE (a.u.)	f_l	Lowest $J=\frac{3}{2}\rightarrow J'=\frac{3}{2}(^2P^0_{3/2})$ ΔE (a.u.)	f_l
5	B	3.824 (−1)	5.844 (−1)	2.475 (−1)	2.563 (−2)	1.113 (−1)	8.676 (−7)
10	Ne^{5+}	1.188	2.205 (−1)	8.394 (−1)	1.003 (−2)	4.280 (−1)	3.109 (−7)
14	Si^{9+}	1.821	1.494 (−1)	1.311	5.799 (−3)	6.876 (−1)	3.255 (−6)
16	S^{11+}	2.148	1.301 (−1)	1.552	4.329 (−3)	8.207 (−1)	7.680 (−6)
18	Ar^{13+}	2.485	1.163 (−1)	1.799	3.089 (−3)	9.568 (−1)	1.560 (−5)
22	Ti^{17+}	3.214	9.849 (−2)	2.315	1.189 (−3)	1.240	4.706 (−5)
23	V^{18+}	3.411	9.537 (−2)	2.449	8.323 (−4)	1.314	5.899 (−5)
26	Fe^{21+}	4.055	8.806 (−2)	2.864	1.468 (−4)	1.541	1.058 (−4)
28	Ni^{23+}	4.538	8.447 (−2)	3.150	1.391 (−6)	1.699	1.459 (−4)
36	Kr^{31+}	7.150	7.696 (−2)	4.361	1.154 (−3)	2.387	3.520 (−4)
42	Mo^{37+}	1.019 (+1)	7.719 (−2)	5.332	2.365 (−3)	2.970	5.069 (−4)
54	Xe^{49+}	2.103 (+1)	8.963 (−2)	7.486	3.525 (−3)	4.344	7.094 (−4)
74	W^{69+}	6.632 (+1)	1.371 (−1)	1.219 (+1)	3.599 (−3)	7.681	8.099 (−4)

The transition between the two J levels of the ground state is forbidden to occur for electric-dipole radiation, but allowed for magnetic-dipole radiation. For this transition, we have used the relativistic form of the transition operator,[1] whose reduced matrix element between two one-electron orbitals with j_f and j_i total angular momenta can be written as

$$\langle \tfrac{1}{2} l_f j_f \| h_{\omega 1} \| \tfrac{1}{2} l_i j_i \rangle = e\sqrt{\hbar\omega}\,(-1)^{j_f+3/2}\frac{(\kappa_f+\kappa_i)}{\sqrt{2}}\sqrt{3}\,[(2j_f+1)(2j_i+1)]^{1/2}\begin{pmatrix} j_f & 1 & j_i \\ \frac{1}{2} & 0 & -\frac{1}{2}\end{pmatrix}\int (F_f G_i + G_f F_i) j_1 dr\,,$$

where κ is as usual equal to $\pm(j+\frac{1}{2})$ for $l=j\pm\frac{1}{2}$, and F and G refer to the large and small components of the Dirac wave function, respectively; the subscripts indicate whether it is the final (f) or the initial (i) state that is being considered. The oscillator strengths and energies of this magnetic-dipole transition are listed in Table IX for the boron isoelectronic sequence.

III. DISCUSSION

In our multiconfigurational wave functions for the ground and excited states, we have included all configurations involving orbitals with $n\leq 2$. These configurations having shells of the same principal quantum number produce intershell-correlation effects, which are expected to dominate the intrashell correlations, at large Z.

TABLE VIII. Energies and oscillator strengths for the transition from $J=\frac{5}{2}$ excited states to ground state of B sequence. Numbers in parentheses are multiplicative powers of ten.

Z	Element \ Transition	Highest $J=\frac{5}{2}\rightarrow J'=\frac{3}{2}(^2P^0_{3/2})$ E (a.u.)	f	Lowest $J=\frac{5}{2}\rightarrow J'=\frac{3}{2}(^2P^0_{3/2})$ E (a.u.)	f
5	B	2.485 (−1)	1.563 (−1)	1.113 (−1)	9.526 (−7)
10	Ne^{5+}	8.396 (−1)	6.315 (−2)	4.312 (−1)	1.209 (−6)
14	Si^{9+}	1.311	4.279 (−2)	7.050 (−1)	1.196 (−5)
16	S^{11+}	1.553	3.701	8.532 (−1)	2.894 (−5)
18	Ar^{13+}	1.804	3.270 (−2)	1.012	6.255 (−5)
22	Ti^{17+}	2.342	2.674 (−2)	1.372	2.316 (−4)
23	V^{18+}	2.487	2.560 (−2)	1.471	3.092 (−4)
26	Fe^{21+}	2.965	2.269 (−2)	1.797	6.765 (−4)
28	Ni^{23+}	3.329	2.103 (−2)	2.034	1.588 (−3)
36	Kr^{31+}	5.435	1.592 (−2)	3.080	3.271 (−3)
42	Mo^{37+}	8.117	1.417 (−2)	3.903	4.399 (−3)
54	Xe^{49+}	1.826 (+1)	1.494 (−2)	5.677	4.823 (−3)
74	W^{69+}	6.234 (+1)	2.247 (−2)	9.601	4.305 (−3)

TABLE IX. Transition energies and oscillator strengths for the forbidden $M1$ decay of the $2s^22p$; $J=\frac{3}{2}$ level to the $2s^22p$; $J'=\frac{3}{2}$ level of ground state of the boron sequence. Numbers in parentheses are multiplicative powers of ten.

Z	Element \ Transition	$2s^2p$; $J=\frac{3}{2}(^2P^0_{3/2}) \rightarrow 2s^22p$; $J'=\frac{1}{2}(^2P^0_{1/2})$ ΔE(a.u.)	f
5	B	1.978 (−3)	5.746 (−9)
6	C^{1+}	1.225 (−3)	3.617 (−9)
7	N^{2+}	1.505 (−3)	4.450 (−9)
8	O^{3+}	2.416 (−3)	7.145 (−9)
10	Ne^{3+}	6.600 (−3)	1.952 (−8)
12	Mg^{7+}	1.565 (−2)	4.627 (−8)
13	Al^{8+}	2.284 (−2)	6.752 (−8)
14	Si^{9+}	3.234 (−2)	9.558 (−8)
16	S^{11+}	6.014 (−2)	1.777 (−7)
18	Ar^{13+}	1.032 (−1)	3.047 (−7)
22	Ti^{17+}	2.552 (−1)	7.528 (−7)
23	V^{18+}	3.112 (−1)	9.177 (−7)
26	Fe^{21+}	5.363 (−1)	1.579 (−6)
28	Ni^{23+}	7.436 (−1)	2.188 (−6)
29	Cu^{24+}	8.676 (−1)	2.552 (−6)
36	Kr^{31+}	2.235	6.544 (−6)
42	Mo^{37+}	4.378	1.275 (−5)
54	Xe^{49+}	1.314 (+1)	3.777 (−5)
74	W^{69+}	5.373 (+1)	1.493 (−4)
82	Pb^{77+}	8.648 (+1)	2.354 (−4)
92	U^{87+}	1.504 (+2)	3.949 (−4)

A. Wave functions

The relativistic $J=\frac{1}{2}$ and $\frac{3}{2}$ ground-state wave functions are formed from the combination of two and four configurations, respectively, the $2s^22p$ configuration being the major one for both states. As shown in Table I, for the $J=\frac{1}{2}$ state, the mixing coefficient of the $2p^3$ configuration is at most 25% of the weight of the $2s^22p$ configuration and drops off with increasing Z. The decrease is close to $1/Z$ at the beginning of the sequence indicative of the near constancy of the ratio of the Coulomb interaction to the energy difference between the $2s^22p$ and $2p^3$ states. For $Z>20$, however, the coefficient for the $2p^3$ configuration decreases much more rapidly owing to the increased influence of the spin-orbit interaction on the energy splitting of the $2s^22p$ and the $2p^3$ levels. For the $J=\frac{3}{2}$ ground state, the $2s^22p_{3/2}$ configuration has the largest weight as shown in columns 4 to 7 of Table I. The largest mixing coefficient of the three relativistic configurations corresponding to the $2p^3$ nonrelativistic configuration is about 17% of that of the dominant configuration ($2s^22p_{3/2}$) around the neutral end of the sequence and decreases to about 10% for the high stages of ionization. Here again, the trend of decrease in the mixing coefficients of the nonprincipal configuration indicates the decrease in the importance of correlation and increase in that of relativistic effects as stages of higher ionization are reached.

For both the $J=\frac{1}{2}$ and $\frac{3}{2}$ excited $1s^22s2p^2$ states, relativistically there are three configurations while the $J=\frac{5}{2}$ is formed by the linear combination of two configurations. In the case of the $J=\frac{1}{2}$ states, as shown in Table II, for ions with large Z, the ordering of the energies of the three configurations is as expected for relativistic states. Thus, for $Z>22$, the highest-energy state is the one in which the $2s2p^2_{3/2}$ has the largest coefficient, the middle state has $2s2p_{1/2}2p_{3/2}$ as its main configuration and the lowest level is dominantly $2s2p^2_{1/2}$. However, for the lighter ions of the sequence, this ordering no longer holds; because of the overwhelming importance of the electrostatic interaction at low Z, the $2s2p_{1/2}2p_{3/2}$ becomes the dominant configuration for the highest-energy eigenstate of the $J=\frac{1}{2}$ excited state, while the $2s2p^2_{3/2}$ is now dominant for the middle-energy state. This inversion of the levels is produced by an energy-level crossing of the two $2s2p^2_{3/2}$ and $2s2p_{1/2}2p_{3/2}$ pure j-j coupled levels. This crossing of the energy levels for the $2s2p^2_{1/2}$ and $2s2p_{1/2}2p_{3/2}$ configurations occurs in the vicinity of Ti^{17+} and is a result of the interplay of electron-electron interaction and relativistic spin-orbit effects. Another point of interest is that for both the middle- and lowest-$J=\frac{1}{2}$ states, the $2s2p^2_{1/2}$ is the dominant configuration. This is possible because the various $J=\frac{1}{2}$ excited states

are obtained by independent self-consistent calculations and so are not orthogonal to one another. Thus it is not possible to label the states according to the dominance of one or the other of the three configurations involved. Rather, the convention we have chosen, namely, labeling them lowest, middle, or highest according to the total energy eigenvalue, would seem to be the appropriate one.

In the case of the $J=\frac{3}{2}$ excited states, the three configurations have coefficients of comparable magnitude for each of the three levels at the neutral end of the sequence. The state with the highest total energy always has the $2s2p_{3/2}^2$ as its dominant component with one or the other of the two $2s2p_{1/2}2p_{3/2}$ configurations having the next largest coefficient. By Mo^{37+}, the largest mixing coefficient of either of the two secondary configurations has dropped to 21% of that of the main one. The dominance of the $2s2p_{3/2}^2$ over the other two, even at low Z, indicates that for $J=\frac{3}{2}$ states, as opposed to the $J=\frac{1}{2}$ states, the electrostatic interaction is not strong enough to invert the energy level ordering expected from the spin-orbit interaction. For the middle and lowest states, on the other hand, the $2s2p_{1/2}2p_{3/2}$ configurations are more important than the $2s2p_{3/2}^2$ configurations. For the lowest level, the $(2s_{1/2}2p_{1/2};J=1)2p_{3/2}$ configuration always has the largest coefficient, whereas for the middle level, the coefficient for this same configuration begins at low Z by being the largest, and then is overtaken by the $(2s2p_{1/2};J=0)2p_{3/2}$ for ions with $Z>26$. For both of the $J=\frac{5}{2}$ excited states, in the low-Z region, $2s2p_{1/2}2p_{3/2}$ and $2s2p_{3/2}^2$ configurations have coefficients of comparable magnitude. For the heavier ions of the sequence, however, the coupling becomes more purely j-j type and thus, the lowest $J=\frac{5}{2}$ level is mostly $2s2p_{1/2}2p_{3/2}$ and the highest one, predominantly $2s2p_{3/2}^2$. As we shall see in Sec. III B, the relative importance of the different configurations is a determining factor in the magnitude of transition energies and oscillator strengths and the trends they follow as we proceed along the isoelectronic sequence.

B. Transition energies and oscillator strengths

The photon energies of the transitions, or the energy difference between the ground and excited states, as well as the oscillator strengths of the transitions considered are listed in Tables IV–IX for some of the ions of the boron sequence. For the ground state some correlation effect has been taken into account by including the $2p^3$ configuration, but for the excited states, only the different relativistic configurations representing the $2s2p^2$ have been considered. The outer electrons of the ions at low stages of ionization are more loosely bound and thus subject to greater correlation effects than those of the more highly ionized systems. On the other hand, for heavier ions, relativistic effects become increasingly more important. In our calculations, the most significant relativistic effects are treated exactly by the use of Dirac-Hartree-Fock wave functions and relativistic forms of the atom-field Hamiltonian. However, the contribution from correlation effects is limited to that arising from the mixing of the chosen configurations included. Thus, our calculations are best suited for the elements that are more highly ionized. The results listed in Tables IV–IX for the low-Z ions (up to about Ne^{5+}) are not very accurate because of the importance of correlation effects in these systems. In Sec. III C we shall discuss the influence of further correlation effects for the heavier ions of the sequence by studying their influence on the results for Fe XXII in some detail. Meanwhile, in the remainder of this section we shall concentrate on some points of particular interest in the transitions studied and the trends that the f values and the energies follow as we progress along the isoelectronic sequence.

In Table IV we have listed the results for the transitions from $J=\frac{1}{2}$ excited states to $J=\frac{1}{2}$ ground state. The oscillator strengths for the transition from the highest-$J=\frac{1}{2}$ excited state to the $J=\frac{1}{2}$ ground state is the largest out of the three for the low-Z ions and slowly decreases as we go to heavy ions in this sequence. Thus for the light ions, the oscillator strength for the middle $J=\frac{1}{2}$ is smaller than that of the highest $J=\frac{1}{2}$ to the ground-state transition. As we progress along the sequence (after about $Z=13$) the f value for the middle-$J=\frac{1}{2}$ to ground-$J=\frac{1}{2}$ transition increases, peaks for Ti^{17+} and slowly falls off becoming nearly constant for high-Z ions. Therefore, after Ar^{13+}, the f of the middle $J=\frac{1}{2}$ to ground $J=\frac{1}{2}$ is larger than that of the highest $J=\frac{1}{2}$. The curves representing the f values of these two transitions as a function of Z are plotted in Fig. 1 and we see that between $Z=18$ and 22 the two curves cross. Relativistically, this crossing of the magnitudes of the f values can be qualitatively explained by considering the coefficients for the three configurations present in the $J=\frac{1}{2}$ excited states listed in Table II. The $2s2p_{3/2}^2$ cannot directly connect to the $2s^22p_{1/2}$ by the electric-dipole interaction, and so the larger the mixing coefficient for this configuration, the smaller the f value for transition to the $J=\frac{1}{2}$ ground state. For low-Z ions of the boron sequence, the dominant configuration for the middle-$J=\frac{1}{2}$ eigenstate is the

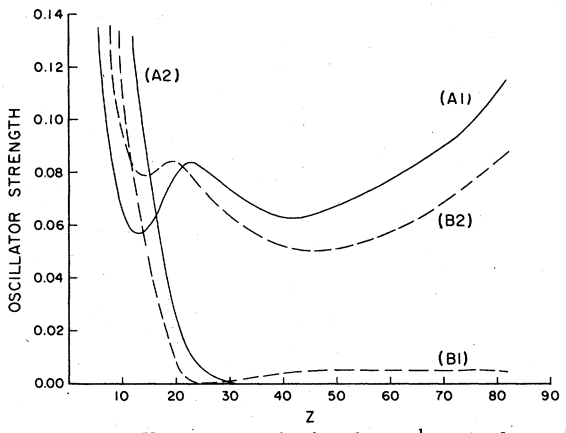

FIG. 1. Oscillator strengths for the $J=\frac{1}{2}$ excited states to the ground-state transitions in B sequence. (A1) and (A2) are transitions from the middle- and highest-$J=\frac{1}{2}$ excited to $J=\frac{1}{2}$ ground state, respectively; (B1) and (B2) are for middle- and highest-$J=\frac{1}{2}$ excited states to $J=\frac{3}{2}$ ground state.

$2s2p_{3/2}^2$, while for the highest $J=\frac{1}{2}$ it is the $2s2p_{1/2}$ $2p_{3/2}$, thus causing the transition from the middle state to have a smaller oscillator strength. For the high-Z region, however, the $2s2p_{3/2}^2$ configuration is increasingly more dominant for the highest eigenstate and less important for the middle one and therefore the oscillator strength for the transition from the middle-$J=\frac{1}{2}$ state to the ground state is much larger than that from the highest state.

For the three transitions from the $J=\frac{1}{2}$ excited state to the $J=\frac{3}{2}$ ground state listed in Table V, on the other hand, it is the $2s2p_{1/2}^2$ configuration which has a vanishing electric-dipole matrix element with the main configuration of the ground state. For the middle-$J=\frac{1}{2}$ state, the coefficient for this configuration, as seen from Table II, increases, goes through a maximum at about $Z=22$ and then decreases along the isoelectronic sequence. As a result, the oscillator strength for the transition from this state to the ground state (Fig. 1) first decreases, goes through a minimum at about $Z=22$, and finally becomes nearly constant. For the highest-$J=\frac{1}{2}$ state, the coefficient for the $2s2p_{1/2}^2$ (Table II) goes through a minimum and so the oscillator strength for the transition between this eigenstate and the $J=\frac{3}{2}$ ground state has a maximum as shown in Fig. 1.

In order to compare our results with nonrelativistic calculations, we have carried out a transformation from j-j to LS coupling for the $J=\frac{1}{2}$ excited states. In Table X we have listed the weights of the LS configurations for a few elements in the boron sequence. By comparing the coefficients listed in columns two and three with those in columns five and six, we observe that up to V^{18+}, the highest eigenstate is predominantly $^2P_{1/2}$ and the middle state $^2S_{1/2}$. After V^{18+}, the situation is reversed, namely, that for the highest state, the dominant coefficient is that of $^2S_{1/2}$ and for the middle state that of $^2P_{1/2}$. This observation is equivalent to the nonrelativistic conclusion[6,7] that the $^2S_{1/2}$ and $^2P_{1/2}$ levels cross in the vicinity of V^{18+}. The curves in Fig. 1 are typical of those for the oscillator strengths of transitions in isoelectronic sequences in the presence of level crossings.[16] In the case of the boron sequence, however, since each excited $J=\frac{1}{2}$ eigenstate is the mixture of three rather than two LS states, the minima in the curves are not as pronounced as in the two-level case.

In the transitions from the lowest-$J=\frac{1}{2}$ excited states to both the $J=\frac{1}{2}$ and $\frac{3}{2}$ ground states, the oscillator strengths start very small and increase along the sequence. These transitions are known as the intercombination lines in the nonrelativistic theory and are allowed as a result of the breakdown of L and S due to the spin-orbit interaction; these therefore become stronger for high Z where relativistic effects are most important.

Excitation energies and oscillator strengths of the transitions from the $J=\frac{3}{2}$ excited states to the ground states are listed in Tables VI and VII. We notice that the oscillator strengths for transitions between the highest $J=\frac{3}{2}$ and both the $J=\frac{1}{2}$ and $\frac{3}{2}$ ground states decrease with increasing Z, while for transitions involving the lowest-$J=\frac{3}{2}$ excited

TABLE X. Conversion from j-j coupling to LS coupling for the three $J=\frac{1}{2}$ excited states of B-like ions.

	Highest eigenstate			Middle eigenstate			Lowest eigenstate		
	$^2P_{1/2}$	$^2S_{1/2}$	$^4P_{1/2}$	$^2P_{1/2}$	$^2S_{1/2}$	$^4P_{1/2}$	$^2P_{1/2}$	$^2S_{1/2}$	$^4P_{1/2}$
Ne^{5+}	−0.999	+0.035	−0.002	+0.029	+0.999	−0.044	0.002	0.008	1.000
S^{11+}	−0.967	+0.257	−0.002	+0.230	+0.973	−0.044	0.009	0.042	0.999
Ti^{17+}	0.773	−0.663	+0.049	+0.626	+0.771	−0.111	−0.031	−0.116	−0.993
V^{18+}	0.737	−0.673	+0.062	+0.671	0.731	−0.124	−0.038	−0.133	−0.991
Fe^{21+}	−0.649	+0.754	−0.104	+0.760	0.628	−0.168	−0.063	−0.188	−0.983
Mo^{37+}	−0.440	+0.842	−0.312	+0.855	+0.286	−0.432	−0.376	−0.474	−0.847

state, the f values increase as we go along the sequence. In the case of the middle-$J=\frac{3}{2}$ states, as shown in Fig. 2, there is a minimum in the curves representing the f values along the sequence at about $Z=26$. These minima can be attributed to a switch in the relative importance of the configurations $(2s2p_{1/2};J=0)2p_{3/2}$ and $(2s2p_{1/2};J=1)2p_{3/2}$ which occurs at about $Z=26$ for the middle-$J=\frac{3}{2}$ eigenstate (Table III).

In Table VIII, transition energies and oscillator strengths of the emission from the $J=\frac{5}{2}$ excited states to the $J=\frac{3}{2}$ ground state are listed. The oscillator strength for the transition from the highest-$J=\frac{5}{2}$ level to the ground state decreases rapidly at first, then more slowly with increasing Z. Around Xe^{49+}, the f value for this transition goes through a shallow minimum and starts to show a slow increase for the very high-Z region. The lowest $J=\frac{5}{2}$ to ground-state transition has a very small oscillator strength a low Z. This can be explained by noting that for the light ions, the lowest-$J=\frac{5}{2}$ level is almost purely equivalent to the nonrelativistic $^4P_{5/2}$ state and this transition corresponds to the weak $^4P_{5/2}$ to $^2P^0_{3/2}$ intercombination line of the nonrelativistic theory. As Z increases, the levels become increasingly j-j coupled and thus, the oscillator strength for the lowest-$J=\frac{5}{2}$ to ground-$J=\frac{3}{2}$ state transition increases rapidly with increasing Z. At $Z=42$, for example, the oscillator strength for the transition between the lowest $J=\frac{5}{2}$ to ground state is 31% of that of the highest $J=\frac{5}{2}$ to ground state. Furthermore, in the oscillator strength of the transition from the lowest $J=\frac{5}{2}$ to the ground state there is a shallow maximum at about $Z=54$, corresponding to the minimum observed in the case of the highest $J=\frac{5}{2}$ to ground-state transition.

The transition between the $J=\frac{1}{2}$ and $\frac{3}{2}$ levels of the ground state proceeds via the magnetic-dipole term in the atom-field Hamiltonian. The energies and oscillator strengths for this $M1$ transition in the boron sequence are listed in Table IX. The f value of this transition is very small for the light ions but increases along the sequence and becomes comparable in order of magnitude to the oscillator strength for some of the weak electric-dipole transitions in the heavy ions. It should be noted here that nonrelativistic theory predicts that the ratio of the oscillator strength to the transition energy will be independent of Z for $M1$ transitions. This is not the case in the relativistic formalism because the radial integral

$$\int (F_j G_{j'} + G_j F_{j'}) j_1 dr$$

present in the magnetic-dipole matrix element [Eq. (1)], is not independent of Z. As shown in Fig. 3, the ratio of f to ΔE as a function of Z is therefore not a nearly horizontal line as the nonrelativistic theory predicts, but a curve whose radius of curvature varies depending upon the region of Z that is considered. These optically forbidden transitions have recently been identified for the medium-Z elements, in tokamak discharges, and applied for localized diagnostics in high-temperature plasmas.[12]

Our results agree in general with those obtained by Cheng *et al.*[9] using MCDHF in the boron sequence. These authors include the nonaverage part of the Breit-interaction and Lamb-shift contributions in evaluating transition energies. Thus, for the very heavy ions their values of the energies are slightly smaller than those obtained in the present work. As for the oscillator strengths,

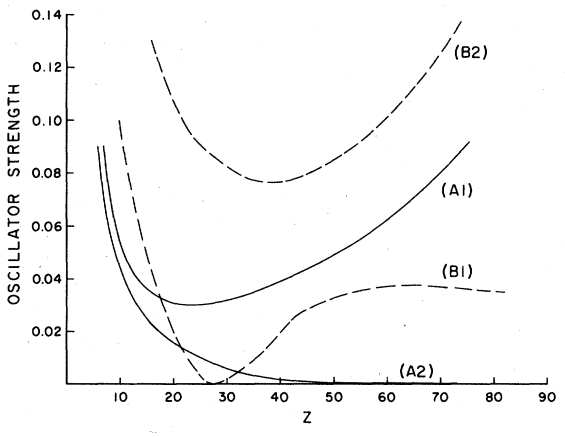

FIG. 2. Oscillator strengths for transitions from $J=\frac{3}{2}$ excited states to ground states of B sequence. (A1) and (A2) are, respectively, for middle- and highest-$J=\frac{3}{2}$ excited states to $J=\frac{1}{2}$ ground state; (B1) and (B2) are for middle- and highest-$J=\frac{3}{2}$ to $J=\frac{3}{2}$ ground state. The curve (B1) represents $10f$ for the transition.

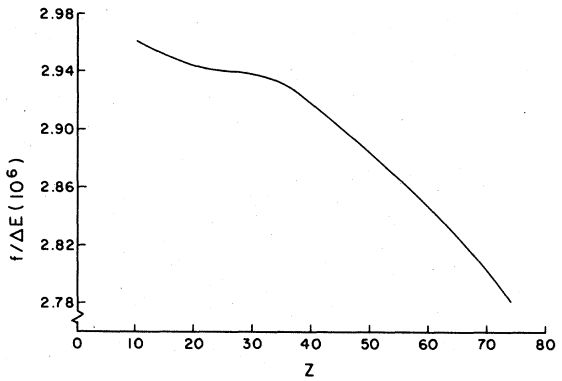

FIG. 3. Relativistic values of $f/\Delta E$ for the $M1$ transitions between the $2s^22p_{3/2}$ and $2s^22p_{1/2}$ ground-state levels of B sequence.

if we convert our emission f_l values to their absorption counterparts, there is also good agreement between our results and those of Cheng *et al.*[9] This is not surprising since, although these authors do not include the exchange-overlap contributions from the core shells mentioned in Sec. II A, these overlap effects are only important for the f_v results and as shall be discussed in Sec. II C, have very little influence on the f_l values.

C. Discussion of results for Fe XXII

As mentioned in Sec. II B, we have carried out a more complete and detailed analysis of the energies and oscillator strengths for transitions in B-like Fe. In this effort, we had two aims: Firstly, to test in one case, ways of improving our results, and secondly, to further understand the importance of the various effects contributing to the transitions in the boron sequency in order to increase our knowledge of the electronic structure of these ions in general. The reason for choosing Fe XXII as the test case was also twofold: First, it is a moderately heavy ion and thus in the intermediate-Z region where both relativistic and many-body effects are important, and second, special interest in Fe in astrophysics and plasma physics has stimulated several calculations for this ion, which will allow us to carry out a detailed comparison with other works. In Table XI, we have listed our values of transition energies and oscillator strengths for the electric-dipole transitions of Fe XXII. Columns two and three, respectively, list the values of the excitation energies and wavelengths of the different transitions obtained by our relativistic multiconfigurational calculation and column four lists the corresponding experimental wavelengths.[17] The agreement is a reasonably good one. The small difference of about 1% can arise from two types of effects: First, the difference between the contributions that intrashell correlation effects make to the ground and excited states, and second, contributions from other energy-shift terms that are not included exactly, such as the nonaverage part of the Breit interaction or the Lamb shift. These effects make contributions that are small relative to the total energies of the states but are nonnegligible to the energy differences. The values of the length and velocity oscillator strength for several transitions between the $2s2p^2$ excited states and ground states are listed in columns five and six of Table XI. The discrepancy between the values obtained by using the two approximations are large and range between 25% of the length value to two orders of magnitude, even at this high level of ionization. Therefore we conclude that even at this level of ionization, many-body effects are important. One type of many-body effect is the contribution to the oscillator strength from the core electrons, namely, the $1s^2$ orbitals in the present case. In columns seven and eight of Table XI, we have listed the values of the oscillator strengths without the exchange-overlap contribution[15] of the $1s$ orbitals for a few transitions. The oscillator strengths evaluated using the relativistic equivalent of the length form are modified at most by 2.0%, while those obtained using the Coulomb gauge (velocity form) change substan-

TABLE XI. Summary of results for $E1$ transitions in Fe XXII.

Transition	$\Delta E_{\text{calc(a.u.)}}$	$\lambda^{\text{calc}}(A^0)$	$\lambda^{\text{expt}}(A^0)$[a]	f_l	f_v	f_l (no overlap)	f_l (no overlap)
Middle $J=\frac{1}{2}\rightarrow J=\frac{1}{2}$	3.944	115.5	117.1	0.802 (−1)	0.482 (−1)	0.810 (−1)	0.710 (−1)
$\rightarrow J=\frac{3}{2}$	3.407	133.7	135.9	0.302 (−4)	0.427 (−2)		
Highest $J=\frac{1}{2}\rightarrow J=\frac{1}{2}$	4.499	101.3	102.2	0.415 (−2)	0.111 (−1)	0.420 (−2)	0.130 (−1)
$J=\frac{3}{2}$	3.962	115.0	116.2	0.714 (−1)	0.321 (−1)		
Lowest $J=\frac{1}{2}\rightarrow J=\frac{1}{2}$	1.834	248.4	246.6	0.796 (−3)	0.183 (−4)	0.799 (−3)	0.458 (−3)
$J=\frac{3}{2}$	1.297	351.3	348.0	0.273 (−3)	0.100 (−3)		
Middle $J=\frac{3}{2}\rightarrow J=\frac{1}{2}$	3.400	134.0	135.7	0.310 (−1)	0.432 (−1)		
$J=\frac{3}{2}$	2.864	159.1	161.6	0.147 (−3)	0.710 (−3)		
Highest $J=\frac{3}{2}\rightarrow J=\frac{1}{2}$	4.591	99.2	100.8	0.943 (−2)	0.634 (−2)		
$\rightarrow\frac{3}{2}$	4.055	112.4	114.4	0.881 (−1)	0.659 (−1)		
Lowest $J=\frac{3}{2}\rightarrow J=\frac{1}{2}$	2.077	219.4	217.3	0.142 (−4)	0.552 (−2)		
$\rightarrow\frac{3}{2}$	1.541	295.7	292.4	0.106 (−3)	0.174 (−3)		

[a] Reference 6.

tially, and in some cases even by an order of magnitude. The fact that the $1s$ exchange-overlap effect influences the two forms of the operator in such a different manner is not surprising since the velocity form of the operator mostly experiences the region near the nucleus and the $1s$ having a large density in this region affects this form considerably. By comparing columns five and six of Table XI on the one hand, and columns seven and eight on the other, we notice that in most cases the two values of f were in better agreement when we had not included the $1s$ overlap contribution. However, even though the length and velocity forms of f agree better without the $1s$ exchange effects for Fe XXII, these contributions are real and must be included in order to give the correct f values for the high-Z limit. This is demonstrated by the curves in Fig. 4 where the f values for the middle-$J=\frac{1}{2}$ excited state to the ground-$J=\frac{1}{2}$ transition are plotted as an example to illustrate this point. When we do include the $1s$ overlap effect, the two curves representing length and velocity smoothly approach each other as we go along the sequence but, without this exchange-overlap contribution, the two curves cross and become further apart in the high-Z region.

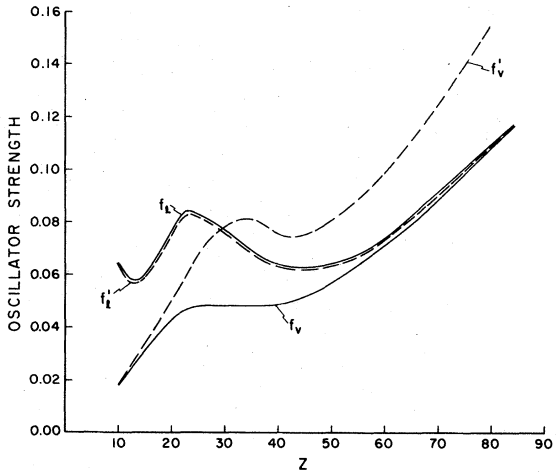

FIG. 4. Comparison of calculated f_l and f_v values neglecting core exchange-overlap contributions (dashed curves) and including core overlap effects (solid curves) for the middle-$J=\frac{1}{2}$ excited state to $J=\frac{1}{2}$ ground-state transition in B sequence.

The next step in trying to improve the transition energies and oscillator strengths for the boron sequence is to examine the effect of additional electron-electron interaction by mixing in more configurations. We attempted this for the middle-$J=\frac{1}{2}$ excited state to the ground state $J=\frac{1}{2}$ transition of the Fe ion. The configurations that we included were all made up of orbitals with $n \leq 3$ and were as follows:

$$\Psi_{\text{ground}} = 2s^2 2p_{1/2} + 2p_{1/2}(2p^2_{3/2}; 0) + (2s\tilde{3}s; 1)2p_{1/2} + (2s\tilde{3}s; 1)2p_{3/2} + (2s2p_{1/2}; 1)\tilde{d}_{3/2} + (2s2p_{3/2}; 1)\tilde{d}_{3/2}$$
$$+ (2s2p_{3/2}; 2)\tilde{d}_{3/2} + (2s2p_{3/2}; 2)\tilde{d}_{5/2} + \tilde{3}s^2 2p_{1/2},$$

$$\Psi_{\text{excited}} = 2s(2p^2_{1/2}; 0) + (2s2p_{1/2}; 1)2p_{3/2} + 2s(2p^2_{3/2}; 0) + (2p_{1/2}\,2p_{3/2}; 1)\tilde{d}_{3/2} + (2p_{1/2}\,2p_{3/2}; 2)\tilde{d}_{3/2}$$
$$+ (2p_{1/2}\,2p_{3/2}; 2)\tilde{d}_{5/2} + (2p^2_{3/2}; 2)\tilde{d}_{3/2} + (2p^2_{3/2}; 2)\tilde{d}_{5/2} + 2s^2\tilde{3}s\,.$$

The orbitals with the tildes over them are pseudo-orbitals. The reason for evaluating the $3s$ orbital of the ground state such that it is coupled to the $2s$ state to give a $J=1$ angular momentum, is to avoid a technical problem present in our relativistic program which prevents us from including two nonfilled orbitals, which have all their quantum numbers except n the same. The $\tilde{d}_j$ orbitals obtained in the calculation are quite similar to $3d_j$ orbitals except near the origin, where an extra node occurs.

In Table XII we list the total energies of the

TABLE XII. Comparison of results obtained for the (middle $J=\frac{1}{2} \rightarrow J=\frac{1}{2}$) transition in Fe XXII by including various numbers of configurations. The numbers in parentheses in the first column represent the number of configurations in the ground state by excited state.

Number of configurations	Final (E_{tot}) (a.u.)	Initial (E_{tot}) (a.u.)	ΔE (a.u.)	f_l	f_v
Smallest set (1×3)		−874.622		8.50 (−2)	4.31 (−2)
Medium set (2×3)	−878.566	−874.622	3.944	8.02 (−2)	4.82 (−2)
Large set (9×9)	−878.569	−874.626	3.943	8.00 (−2)	5.22 (−2)

states, the excitation energy and the length and velocity forms of the oscillator strength for the three cases corresponding to the various number of configurations included in initial and final states. The smallest set refers to the case with $1s^2 2s^2 2p$ configuration in the ground state and $1s^2 2s 2p^2$ in the excited; the medium set in addition, includes $2p^3$ correlation in the ground state. The configurations included in the large set are listed in the expressions for Ψ_{ground} and Ψ_{excited} above. Comparing the results from the largest set with those obtained by only including configurations having $n=2$, namely, the medium size set, we see that f_l is decreased by only about 0.4% while f_v is increased by 7.7% and thus the net gap between the two is diminished to 35% of the length-form value of the oscillator strength. This improvement is disappointing since, in calculations in other isoelectronic sequences, it was found that by including configuration with $n' \leq n+1$, where n is the principal quantum number of the outermost shell of the main configuration involved in the transition, the gap between the length and velocity forms was almost completely bridged. It is not understood why the boron sequence does not follow the previously established norm. However, what is clearly happening is that the length form is hardly affected by the different modifying effects such as correlation and exchange overlap, while the velocity form is quite unstable. This leads us to believe that the value obtained for f using the length form of the operator is more reliable and that eventually, the velocity form will converge to it, provided one includes all the possible physical effects. One possible effect which might influence the velocity form is the core polarization of the $1s$ electrons where configurations such as $1s2s^2 3s2p_{1/2}$, will have to be included in the ground-state wave function. This effect may indeed have a large contribution since the exchange-overlap effect, because it involved $1s$ electrons with large densities near the nucleus, modified the velocity oscillator strength considerably. Several attempts have been made to incorporate core-polarization effects in the evaluation of atomic properties[8,18]; we shall also try to include this effect in evaluating the oscillator strength of transitions in the B sequence and will report on that effort in the future. Finally in Table XIII we list our results obtained for the excitation energies and length-form oscillator strengths of several transitions in Fe XXII, along with those obtained by other authors using various methods, for comparison purposes. The transition energies obtained using the relativistic MCHF procedure (columns two and four of Table XIII), are in good agreement with the experimental results[17] and are in reasonable agreement with the energies obtained[7] by the configuration-interaction method. Also, comparing columns six, seven, and eight of Table XIII, we find that our values of the oscillator strength of the various transitions obtained by using the relativistic gauge equivalent of the length form agrees with two nonrelativistic calculations[6,7] of f_l.

TABLE XIII. Comparison of results for energies and oscillator strengths of transitions in Fe XXII. Numbers in parentheses are multiplicative powers of ten.

Transition	ΔE(a.u.)[a]	ΔE(a.u.)[b]	ΔE(a.u.)[c]	ΔE_{expt}(a.u.)[d]	f_l[a]	f_l[b]	f_l[e]
$J=\frac{1}{2} \rightarrow$ Middle $J=\frac{1}{2}$	3.944	3.877	3.928	3.891	0.80 (−1)	0.80 (−1)	0.79 (−1)
Middle $J=\frac{3}{2}$	3.400	3.339	3.380	3.358	0.62 (−1)	0.59 (−1)	0.59 (−1)
Highest $J=\frac{1}{2}$	4.499	4.439	4.490	4.458	0.45 (−2)	0.30 (−1)	0.3 (−1)
Highest $J=\frac{3}{2}$	4.591	4.496	4.570	4.520	0.20 (−1)	0.19 (−1)	0.19 (−1)
$J=\frac{3}{2} \rightarrow$ Middle $J=\frac{1}{2}$	3.407	3.351	3.390	3.353	0.15 (−4)	0.2 (−3)	0.2 (−3)
Middle $J=\frac{3}{2}$	2.864	2.814	2.841	2.820	0.15 (−3)	0.1 (−3)	0.1 (−3)
Highest $J=\frac{1}{2}$	3.962	3.914	3.952	3.921	0.36 (−1)	0.34 (−1)	0.34 (−1)
Highest $J=\frac{3}{2}$	4.055	3.970	4.032	3.983	0.88 (−1)	0.88 (−1)	0.88 (−1)

[a] Present work. For the sake of comparison, emission oscillator strengths are converted to their absorption counterpart.

[b] Reference 7.

[c] Reference 9. In this calculation the Breit interaction and the Lamb shift are treated exactly in first-order perturbation theory (not in an average way) and thus the transition energy is improved. Our values of the oscillator strengths and those of Ref. 9 are in good agreement, and thus we only list our f_l values.

[d] Reference 17.

[e] Reference 6.

IV. CONCLUSIONS

We have evaluated oscillator strengths and transition energies for the electric-dipole transitions between $1s^22s2p^2$ and $1s^22s^22p$ levels, and for the magnetic-dipole transition between two J levels of $1s^22s^22p$, in the B-isoelectronic sequence. Since the transitions studied are all $\Delta n=0$, relativistic effects are crucial and have been included in a first principle manner in the following two ways: (a) Relativistic wave functions obtained by the Dirac-Hartree-Fock procedure are used which automatically take into account effects such as the breakdown of LS coupling and (b) the relativistic form of the atom-field Hamiltonian is used for obtaining expressions for the electric- and magnetic-interaction operators. The first effect is the one predominantly responsible, for example, for the transitions corresponding to the nonrelativistic intercombination lines. One example of the importance of the second is the fact that the ratio of $f/\Delta E$ is not constant for $M1$ transitions along the sequence.

Furthermore, in the present work, by studying the results as a function of Z, along the isoelectronic sequence, we observed several interesting trends which were discussed in Sec. III. These trends (the level crossing of the $^2S_{1/2}$ and $^2P_{1/2}$ excited states, for example) are a direct consequence of the interplay of relativistic and electron-electron interaction effects and were observed owing to the first principle nature of our procedure which treats relativistic and many-body effects on an equal footing. The transition energies obtained by using the relativistic multiconfiguration procedure are in good agreement with the available experimental data. We also calculated oscillator strengths of $E1$ transitions using two relativistic gauges. Correlation effects are responsible for the two values obtained for f from the two gauges. Even though we have included all intershell correlations, f_l and f_v agree with each other only in high-Z elements for the various transitions, and a rather large discrepancy between them exists at low- and intermediate-Z regions of the sequence. We have tried to improve our results for a test case, namely, the middle-$J=\frac{1}{2}$ excited state to $J=\frac{1}{2}$ ground state of Fe^{22+}. Including most of the $\Delta n=1$ correlating configurations in the ground and excited states improves the agreement, by increasing the f_v value, but still leaves a significant gap. We also found that the value of f_v changes considerably due to the influence of the $1s$ core-exchange contribution along the isoelectronic sequence. We thus conclude that since added correlation and core effects have little influence on the oscillator strengths calculated using the length equivalent gauge, this form of the operator is the more stable one. We expect that including further many-body effects involving the valence and core shells, will modify the value of the velocity form of the oscillator strength and bring it closer to the length value for low- and medium-Z elements.

ACKNOWLEDGMENT

This work was supported by the U. S. Department of Energy under Contract No. DE-AS02-76ET53006.

*Present address: Department of Physics, East Carolina University, Greenville, N. C. 27834.

[1]L. Armstrong, Jr., in *Topics in Current Physics*, Vol. 5, edited by I. A. Sellin (Springer, Berlin, 1978); I. P. Grant, J. Phys. B 7, 1458 (1974).

[2]L. Armstrong, Jr., W. R. Fielder, and Dong L. Lin, Phys. Rev. A 14, 1114 (1976).

[3]C. D. Lin and W. R. Johnson, Phys. Rev. A 15, 1046 (1977); Y.-K. Kim and J. P. Desclaux, Phys. Rev. Lett. 36, 139 (1976); G. A. Martin and W. L. Wiese, Phys. Rev. A 13, 699 (1976).

[4]Dong L. Lin, W. Fielder, Jr., and Lloyd Armstrong, Jr., Phys. Rev. A 16, 589 (1977); William Fielder, Jr., Dong L. Lin, and Dinh Ton-That, *ibid.* 19, 741 (1979).

[5]A. W. Weiss, Phys. Rev. 188, 119 (1969).

[6]W. Dankwort and E. Trefftz, J. Phys. B 10, 2541 (1977); Astron. Astrophys. 65, 93 (1978).

[7]R. Glass, J. Phys. B 13, 15 (1980); 13, 899 (1980).

[8]J. Migdalek and W. E. Baylis, in *Abstracts of the 7th International Conference on Atomic Physics* (M.I.T., Cambridge, 1980).

[9]K. T. Cheng, Y.-K. Kim, and J. P. Desclaux, At. Data Nucl. Data Tables 24, 111 (1979).

[10]*Beam-Foil Spectroscopy*, edited by I. A. Sellin and D. J. Pegg (Plenum, New York, 1976); *Beam-Foil Spectroscopy*, edited by S. Bashkin (Gordon and Breach, New York, 1968).

[11]A. K. Dupree, Adv. At. Mol. Phys. 14, 393 (1978); D. R. Flower and H. Nussbaumer, Astron. Astrophys. 45, 145 (1975); A. H. Gabriel and C. Jordan, Case Stud. At. Coll. Phys. 2, 211 (1972).

[12]S. Suckewer, R. Fonck, and E. Hinnov, Phys. Rev. A 21, 924 (1980); E. Hinnov, in *Diagnostics for Fusion Experiments*, edited by E. Sindoni and C. Wharton (Pergamon, New York, 1979); C. Breton, D. DeMichelis, and M. Mattioli, J. Quant. Spectrosc. Radiat. Transfer 19, 369 (1978).

[13]J. P. Desclaux, Comput. Phys. Commun. 9, 31 (1975).

[14]I. P. Grant, Adv. Phys. 19, 747 (1970).

[15]P. O. Lowdin, Phys. Rev. 97, 1474 (1955); K. T. Cheng and W. R. Johnson, Phys. Rev. A 15, 1326

(1977).
[16]C. Froese-Fischer, Phys. Rev. A 22, 551 (1980).
[17]B. C. Fawcett, At. Data Nucl. Data Tables 14, 177 (1974).
[18]C. Froese-Fischer, J. Phys. B 10, 1241 (1977); D. W. Norcross, Phys. Rev. A 7, 606 (1972); J. C. Weisheit, *ibid.* 5, 1621 (1972); S. Hameed, A. Herzenberg, and M. G. James, J. Phys. B 1, 822 (1968).